

REMOVAL OF LEAD IONS BY NIFE₂O₄ NANOPARTICLES

V. Andal¹, G. Buvaneswari²

¹KCG College of Technology, Karapakkam, Chennai-100

²Materials Chemistry Division, School of Advanced Sciences, VIT University, Vellore – 632 014, Tamil Nadu, India

Abstract

Nickel ferrite nanoparticles have been prepared by polymeric precursor method. The nanoparticles application in the removal of lead ion was investigated. The results showed that the adsorptive properties were dependent on pH, duration and temperature. Highest percentage (99%) lead adsorption was observed under basic condition at room temperature during 1 h stirring. Analysis of lead adsorbed nickel ferrite by powder XRD, FTIR and XPS techniques revealed the adsorption took place based on hydroxide mechanism. The lead salt formed on the surface of the ferrite powder was identified to be lead carbonate and lead hydroxy carbonate at pH 7 and 9 respectively.

Keywords: Nickel ferrite; Nanoparticles; Lead; Adsorption; Hydroxide

-----***-----

1. INTRODUCTION

Adsorption process has been used for the removal of solutes from solution and gases from the atmosphere. The extent of adsorption depends on the surface area and the porosity of the adsorbent. A better adsorbent possess larger surface area and takes lesser time for efficient adsorption. The adsorption technique in the removal of heavy metal ions from wastewater plays an important role from environmental point of view. Magnetic adsorbents have been used for the waste treatment applications. Recently, there has been a considerable interest shown in using iron oxides for the removal of lead ions from wastewater [1]. Among the magnetic adsorbents ferrites are potential candidates for the separation of hazardous metals such as cadmium, lead, mercury and actinides from waste water [2]. In addition, metal oxide nanoparticles are ideal adsorbents for heavy metal ions due to the larger surface area accomplished by the smaller particle size in comparison to bulk materials [3].

Iron oxides treatment for the removal of trace metal ions from wastewater is more advantageous because the adsorbent can easily be separated from the solution by magnetic means. Some of the reports of iron oxides as adsorbents include adsorption of lead [4], removal of selenite [5], removal of arsenite [6], removal of mercury [7] and removal of neutral red dye [8]. Different ferrite spinel nanoparticles such as NiFe₂O₄, MnFe₂O₄, CoFe₂O₄ and MgFe₂O₄ have been studied as adsorbents for sulphur, dyes and sulphur dioxide [9-12]. Nickel ferrite has been widely studied as a magnetic, catalytic and gas sensing material but reports associated to its adsorption properties are limited [13-15].

Lead is a toxic element released to the environment by various sources. The permissible level for lead in drinking water is 0.005 mg/L [ISI (1982) Tolerance limits for Industrial

effluents prescribed by Indian standards Institution; IS: 2490 (Part II), New Delhi, India]. The permissible limit for lead in waste water given by the Environmental Protection Agency (EPA) is 0.015 mg/L, and that of the Bureau of Indian Standards (BIS) is 0.1 mg/L [16]. Lead ion pollution is mainly due to wastewaters of mining industries, paints and pigment industries, fertilizer industries, metal plating industries, batteries and tannery industries [17]. Lead accumulation causes various diseases to living organism. Lead toxicity in human leads to disruption of the biosynthesis of haemoglobin, rise in blood pressure, kidney damage, miscarriages and abortions, brain damage and learning disabilities in children [18]. Commonly used methods for the removal of lead from aqueous solutions are chemical precipitation, co-precipitation, adsorption, flocculation, reverse osmosis, ion exchange, electro deposition and filtration [16]. Most of these methods have several disadvantages such as chemical requirements, time consuming procedure, production of large amount of sludge, low efficiency and less cost effective [19]. However, adsorption method is considered to be more efficient, cost effective and free from sludge formation. A variety of metal oxides used for the removal of lead are NiO [20], ZnO, CuO, Co-Fe₂O₃ [21], α -Al₂O₃ [22] and Y₂O₃ [23]. Among the metal oxide adsorbents, iron oxide based materials are found to be efficient and industry friendly due to the large surface to volume ratio and the advantage of magnetic separation from wastewater [1]. Oxides such as γ -Fe₂O₃ and Fe₃O₄ have been studied as adsorbents for Pb²⁺ ion [24, 25].

From the reported results it is noted that the iron oxides exhibit less efficiency in the removal of lead ion from aqueous solution [4, 21]. In order to achieve improved percentage removal in a shorter duration, current study explores the application of nano nickel ferrite powder as an adsorbent. The

influence of the factors such as pH, temperature and time has been investigated.

2. EXPERIMENTAL

2.1. Materials

A. R grade Nickel Chloride, Ferric Chloride and Lead acetate purchased from Qualigens and Alginic acid (19-25%) from Sd fine chem. Ltd. were utilized

2.2. Synthesis of NiFe₂O₄

The compound was prepared by polymeric precursor method using alginic acid. Nickel Chloride (1M) and Ferric Chloride solutions (1M) were prepared and mixed in 1:2 volume ratio. To the homogenized solution, alginic acid solution of the concentration 10% by weight was added. The gel formed was dried to get precursor. The dried precursor was calcined at various temperatures in the range 100-1000°C to obtain pure NiFe₂O₄. At each temperature the sample was heated for 6 h.

2.3. Adsorption Study on NiFe₂O₄

For the adsorption experiment, 0.25 g of spinel powder was introduced into 25 ml of lead acetate solution (0.01 M). After adjusting the pH to 7 the ingredients were stirred (170 rpm) at room temperature (29° C). After 12 h the solution was eluted using Whatmann filter paper (125 mm) and preserved for atomic absorption study. The solid (adsorbent) was washed with distilled water and air dried. Similar experiment has been performed under basic (pH=9) condition and at 50° C. The room temperature experiment was performed for duration of 1 h also.

2.4. Characterization

NiFe₂O₄ and lead adsorbed NiFe₂O₄ samples were characterized by powder X-ray diffraction method (Cu K_α, D8 Advance, Bruker). The average particle size was determined using Scherrer formula. The Infrared spectra (FTIR spectrometer, model JASCO 4100) were recorded using KBr disc technique. Scanning Electron Microscopic analysis of the samples was carried out using FEI QUANTA FEG 200 HR Scanning Electron Microscope. The XPS spectra were recorded using ESCA model VG3000 system.

3. RESULTS AND DISCUSSION

3.1 Characterisation of NiFe₂O₄ before and after Adsorption

3.1.1 Powder X-ray Diffraction Analysis

Powder XRD patterns compiled in Fig.1 indicate the gradual change in the precursor on heating at various temperatures and confirm the formation of pure and highly crystalline spinel oxide at 1000°C. With rise in temperature the intensity of the

peaks corresponding to Fe₂O₃ (2θ = 24.21°, 33.05°, 40.94°) reduces and at 1000° C these peaks completely disappear. The diffraction pattern (Fig.1d) is in good agreement with the reported data (JCPDS card no: 74-1913) of NiFe₂O₄. The compound crystallises in cubic structure and the lattice parameter calculated is 8.30 Å. The average particle size calculated from the Scherrer formula is 78 nm.

In Fig.2, the XRD patterns of lead adsorbed NiFe₂O₄ nanoparticles at different pH conditions (7 and 9) for 1 h experiment are compiled. Besides the characteristic peaks of NiFe₂O₄, the new peaks found are due to the formation of PbCO₃ and Pb₃(CO₃)₂(OH)₂ [JCPDS file 13-0131] [26]. The nature of the lead compound formed varies as the pH varies from 7 to 9. At pH = 7 the lead compound formed on the surface is lead carbonate and at pH = 9, lead carbonate hydroxide is observed. The residue obtained after the adsorption experiment under pH = 9 condition was washed with dilute acid and water. Powder XRD pattern (Fig. 2) of the resultant dried powder confirms the regeneration of the parent compound.

3.1.2. Infrared Spectroscopic Analysis

Infrared spectroscopy is used to study the interaction of the NiFe₂O₄ with the lead ions. FTIR spectra recorded in the region of 4000-400 cm⁻¹ for NiFe₂O₄ and lead adsorbed NiFe₂O₄ at two different pH conditions are shown in Fig.3. The FTIR spectrum of NiFe₂O₄ (Fig.3 (a)) shows the characteristic peaks of Fe-O and NiO at 597 (ν₁) and 404 (ν₂) cm⁻¹. The absorption band (ν₁) is attributed to Fe in tetrahedral site and (ν₂) is assigned to octahedral site accommodating Ni [27].

The spectra of lead adsorbed NiFe₂O₄ at pH = 7 and 9 show bands at 1400 cm⁻¹ and 1633 cm⁻¹ indicating hydroxide and carbonate groups. It is inferred that there is formation of lead carbonate [28] and lead hydroxide [29] (amount is too less to be identified from the powder XRD pattern-Fig. 2a) at pH = 7. In the spectrum Fig 3c, presence of the bands corresponding to hydroxy and carbonate groups confirms the formation of the compound Pb₃(CO₃)₂(OH)₂ [29] as determined from the powder X-Ray diffraction.

3.1.3. X-ray Photoelectron Spectroscopic Analysis

More information regarding the state of the surface adsorbed lead ion is obtained from XPS analysis. Fig .4 compares the Pb 4f peaks of the products formed on the surface of NFO at different pH conditions. The Pb 4f spectra of the products possess two broad singlet peaks corresponding to Pb 4f_{7/2} and Pb 4f_{5/2} centered around binding energy values 138.5 eV and 143 eV respectively. This observation confirms the oxidation state of lead as Pb²⁺ [30-33].

The O1s spectra compiled in Fig. 5 further confirms the carbonate and hydroxy carbonate formation. The B.E value

529.3 eV of Fig 4b (spectrum (i)) represents O 1s of carbonate group [34] and 530.9 eV of Fig 4b (spectrum (ii)) corresponds to that of hydroxy group of lead hydroxy carbonate [35]. But the ratio of formation of carbonate and hydroxy carbonate is found to be dependent on the pH condition. Neutral condition favours the carbonate formation and as the pH increases hydroxy carbonate forms. Similar, observation is reported by Tang et al [26].

3.1.4. SEM Analysis

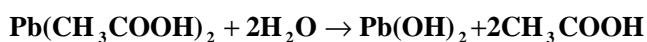
SEM image of NFO powder (Fig. 6) shows the formation of nanosized particles as determined from powder X-Ray diffraction data. The EDAX spectra given in Fig. 7b confirm the adsorption of lead on the surface of NFO at pH = 9.

3.2. Effect of pH, Time and Temperature

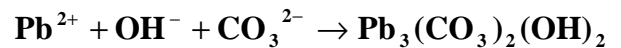
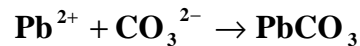
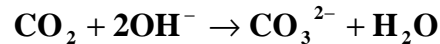
The results obtained by varying the pH, contact time and temperature are given in Table 1. The lead adsorption is found to be efficient under basic condition. For a given pH, the contact time influences the percentage adsorption. Higher percentage and nearly complete adsorption (99 %) is noticed at pH = 9 during 1h contact time. The reduction in the percentage adsorption with longer duration (12 h) could be due to a possible diffusion or dissolution of the lead salts formed on the surface of NFO. Based on the results, it is envisaged that the surface charge of NiFe₂O₄ (NFO) is modified with pH variation. An increase in pH increases the surface negative charge which in turn influences more and more adsorption of lead ions (Fig. 8). Powder XRD, FTIR and XPS results demonstrate that the surface negative charge is created by OH⁻ and CO₃²⁻ ions. The OH⁻ ion comes from the aqueous medium and CO₃²⁻ ion forms due to the interaction of atmospheric CO₂ with OH⁻ in the medium [29]. Effect of rise in temperature is studied at pH = 9 and it is noticed that elevated temperature destroys the lead adsorption (Table.1).

3.3. Adsorption Mechanism

Metal ions get adsorbed on the surface of adsorbent either by ion exchange or complex formation between the functional groups on the surface of the adsorbent and the metal ions [3, 30]. In the current system, no such ion exchange between NiFe₂O₄ and Pb²⁺ or complex formation is observed. The similarity of the powder XRD pattern recorded after the desorption of the lead from the surface of NFO (pH = 9) by dilute acid treatment confirms that there is no ion exchange between NFO and the lead ion. Similarly, since NFO surface is not functionalized by any groups such as thiol, lead adsorption by complex formation is also ruled out. Powder XRD and XPS analysis confirm hydroxide mechanism. The concentration of OH⁻ ion varies with pH and this influences the amount of lead hydroxide formation. The following sequence of reactions could be considered [29]



CO₂ from the atmosphere forms CO₃²⁻ ion on reacting with OH⁻ [29]



Results obtained in the current investigation are compared with that of the literature reports. Nanosized γ-Fe₂O₃ and its complex composite exhibit 15 and 50 % efficiency in removing lead ion in 12 h duration [4]. Similarly, the efficiency achieved in using γ-Fe₂O₃ synthesized by microwave method is around 39 % [24]. Co-Fe₂O₃ also shows very less adsorption (9 % removal during 12 h) [21]. Recillas et al reported 83 mg Pb adsorption per gram of Fe₃O₄ nanoparticles [36]. The current work reports 99 % efficiency in the removal of lead ion at room temperature under basic condition (pH = 9) during 1h. The adsorption capacity of NiFe₂O₄ is determined to be 168 mg/g of NFO.

CONCLUSIONS

Nickel ferrite, NiFe₂O₄ nanoparticles prepared by polymeric precursor method has been applied to remove lead ions from aqueous solution. Adsorption efficiency under neutral and basic (pH = 9) conditions has been studied. It is observed that longer duration and elevated temperature (50° C) lead to lesser adsorption. The oxide removes 99 % of lead at room temperature (29° C) under basic condition during one hour contact. Examination by X-ray diffraction and spectroscopic techniques reveal that lead gets adsorbed on the surface of the ferrite due to the accumulation of negative charge on the surface and forms lead hydroxide and carbonate. The easily separable spinel nanoferrite is regenerated by gentle dilute acid wash.

ACKNOWLEDGEMENTS

The authors thank VIT University for providing all required facilities to carry out the experiments.

REFERENCES

- [1]. Z.Cheng, A.L.K.Tan, Y.Tao, D.Shan, K.E.Ting, X.J.Yin, Int. J Photoenergy. 2012 (2012) 1-5.
- [2]. J.D.Navratil, J. Radioanal. Nucl. Chem. 248 (2001) 571-574.
- [3]. N. Savage, M. S. Diallo, J. Nanopart. Res. 7 (2005) 331-342.
- [4]. N.N. Mallikarjuna, A.Venkataraman, Talanta. 60 (2003) 139.

[5]. C.M. Gonzalez, J. Hernandez , J. R. Peralta-Videa, C. E. Botez, J. G. Parsons, J. L. Gardea- Torresdey, J. Hazard. Mater. 211-212 (2012) 138-145.

[6]. B. Prasad, C. Ghosh, A.Chakraborty, N. Bandyopadhyay, R.K. Ray, Desalination. 274 (2011) 105-112.

[7]. P.I. Girginova, P. I., A. L. Daniel-da-Silva, C. B. Lopes, P. Figueira, M. Otero, V. S. Amaral, E. Pereira, T. Trindade, J. Colloid Interface Sci. 345 (2010) 234-240.

[8]. M.Iram, C. Guo, Y. Guan, A. Ishfaq, H. Liu, J. Hazard. Mater. 181 (2010) 1039-1050.

[9]. N.M. Deraz, A.Alarifi, S.A.Shaban, J. Saudi Chem.Soc. 14 (2010) 357-362.

[10]. R.Wu and J. Qu, J. Chem. Technol. Biotechnol. 80 (2005) 20-27.

[11]. T.G.Glover, D. Sabo, L. A. Vaughan, J. A. Rossin, Z. J. Zhang, Langmuir. 28 (2012) 5695-5702.

[12]. L.Zhao, X. Li, Q. Zhao, Z. Qu, D. Yuan, S. Liu, X. Hu, G.Chen, J.Hazard. Mater. 184 (2010) 704-709.

[13]. L.Chen, H. Dai, Y. Shen, J. Bai, J. Alloys Compd. 491 (2010) L33-L38.

[14]. D.Guin, B. Baruwati, S. V. Manorama, J. Mol. Catal. A: Chem. 242 (2005) 26-31.

[15]. C.Xiangfeng, J. Dongli, Z. Chenmoum, Sens. Actuat. B.123 (2007) 793-797.

[16]. N. Li, R. Bai, Ind. Eng. Chem. Res. 45 (2006) 7897-7904.

[17]. K.Jayaram, M.N.V. Prasad, J.Hazard.Mater. 169 (2009) 991-997.

[18]. N.R.Axtell, S.P.K.Sternberg, K.Claussen, Bioresour. Technol. 89 (2003) 41-48.

[19]. V.K.Gupta, S.Agarwal,T.A.Saleh, J.Hazard.Mater. 185 (2011) 17-23.

[20]. A.Naeem, M.T. Saddique, S. Mustafa, Y. Kim, B. Dilara, J.Hazard.Mater.168 (2009) 364-368.

[21]. A.Lagashetty, M.Bedree and A.Venkataraman, J. Met.Mater Sc. 52 (2010) 357-362.

[22]. S.Naeem, N. Zahra, U. Zafar and S. Munawar, Bangladesh J.Sci.Ind.Res. 44 (2009) 403-406.

[23]. S.Sadjadi, S.J.Ahmadi, M.Hosseinpour, J. Nano Res.16 (2011) 83-87.

[24]. A. Lagashetty, H.Vijayanand, S.Basavaraja, N.N.Mallikarjuna, A.Venkataraman Bull. Mater. Sci. 33 (2010) 1-6.

[25]. N. N. Nassar, J. Hazard. Mater. 184 (2010) 538-546.

[26]. Z.Tang, S. Hong , W. Xiao , S. Seal , J. Taylor, Corros. Sci. 48 (2006) 3413-3427.

[27]. M. Srivastava, S.Chaubey, A.K.Ohja, Mat. Chem. Phy. 118 (2009) 174-180.

[28]. M.S. Refat and K. M .Elsabawy, Bull.Mater. Sci. 34 (2011) 873-881.

[29]. S. Li, W. Yang, M. Chen, J. Gao, J. Kang, Y. Qui, Mat. Chem. Phy. 90 (2005) 262-269.

[30]. V.J.Inglezakis, M.A.Stylianou, D.Gkantzou, M.D. Loizidou, Desalination. 210 (2007) 248-256.

[31]. A .Swiatkowski, M. Pakula, S.Biniak, M.Walezky, Carbon. 42 (2004) 3057-3069.

[32]. A.Godelitsas, J.M. Astilleros, K. Hallam, S. Harissopoulos, A. Putnis, Environ. Sci. Technol. 37(2003) 3351-3360.

[33]. L.R.Pederson, J. Electron Spectrosc. Relat. Phenom. 28 (1982) 203-209.

[34]. P.Nowak, K. Laajalehto, Physicochem. Probl .Mi. 41(2007) 107-116.

[35]. X.Zhang, S.Lin, Z.Chen, M.Megharaj, R.Naidu, Water. Res, 45 (2011) 3481-3488.

[36]. S.Recillas, A. Garcia, E.gonzalez, E.Casals, V.Puntes, A.Sanchez, X.Font, Desalination. 277 (2011) 213-220.

Table 1 Effect of temperature, time and pH on the % adsorption of lead

Temperature (° C)	Time	pH	
		7	9
29	12 h	73	77
	1 h	79.5	99
50	12h	---	23

FIGURE CAPTIONS

Fig.1. Powder X-ray diffraction patterns of the products formed at different temperatures (a) 700° C, (b) 800° C, (c) 900° C and d) 1000° C (*-Fe₂O₃)

Fig 2 Powder XRD patterns of ‘Pb’ adsorbed NiFe₂O₄ nanoparticles at different pH conditions for 1h adsorption and the spinel oxide collected after desorption

Fig 3 FTIR spectra of (a) parent NiFe₂O₄ and Pb adsorbed (1h duration) NiFe₂O₄ at (b) pH=7, (c) pH=9

Fig 4 The Pb (4f) XPS peaks of NiFe₂O₄ after adsorption of lead

Fig 5 The O (1s) XPS peaks of NiFe₂O₄ after adsorption of lead

Fig 6 SEM image of NiFe₂O₄

Fig 7 EDAX spectra of (a) NiFe₂O₄ and (b) Pb adsorbed NiFe₂O₄

Fig 8 Schematic representation of the adsorption process at pH =7 and 9

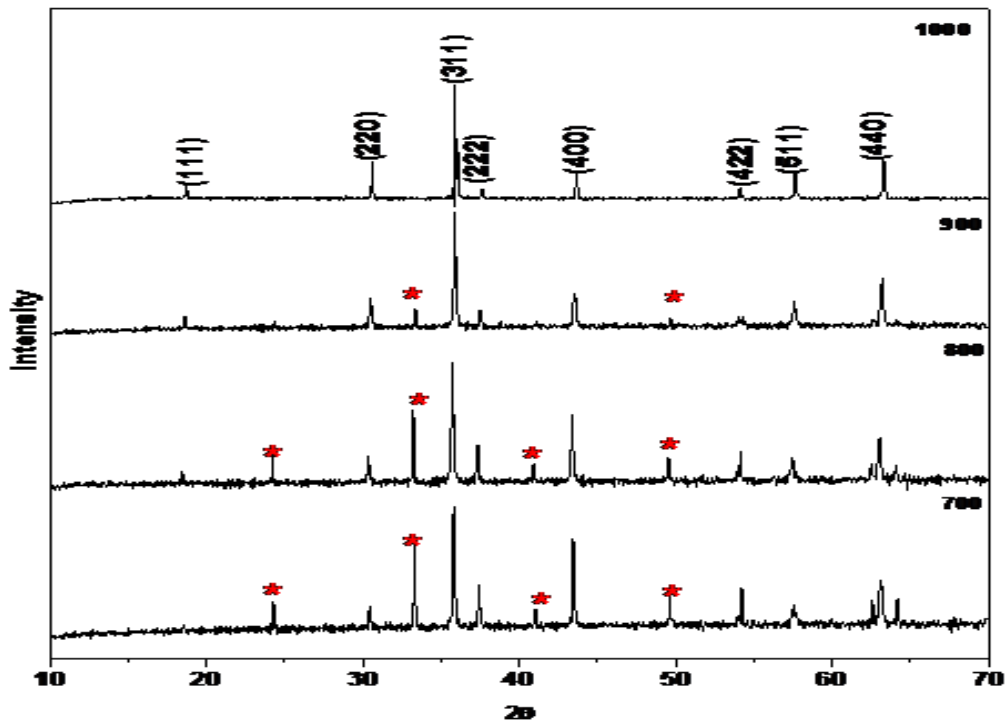


Fig 1

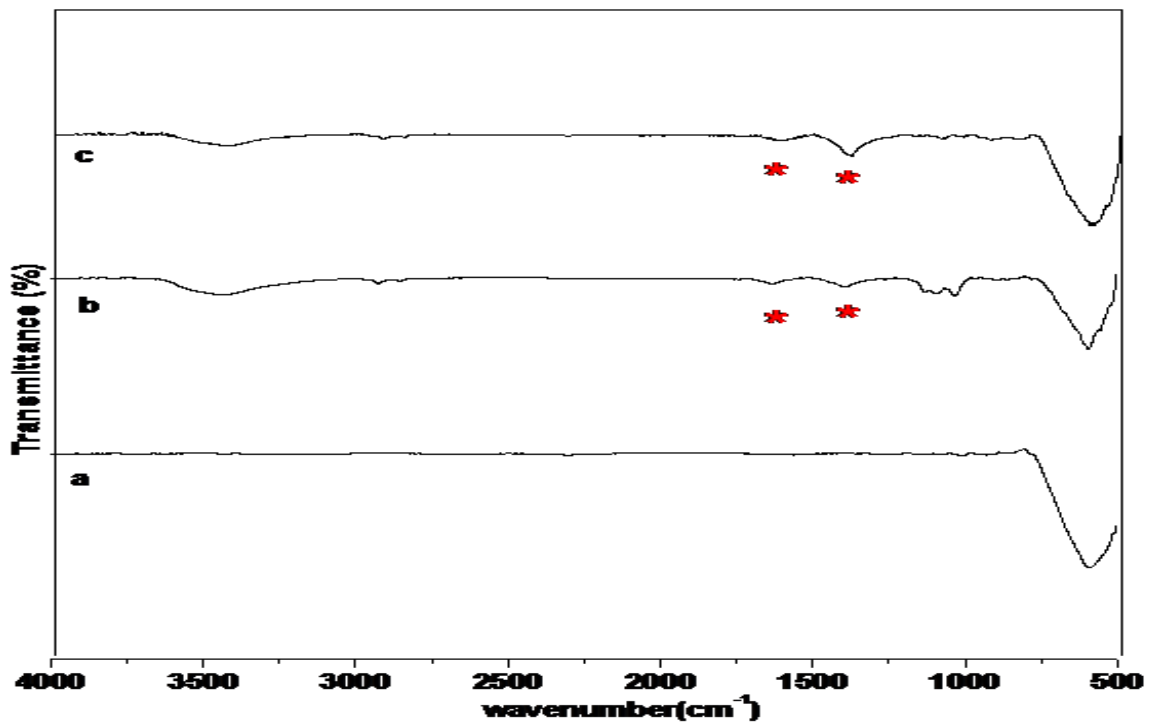


Fig 2

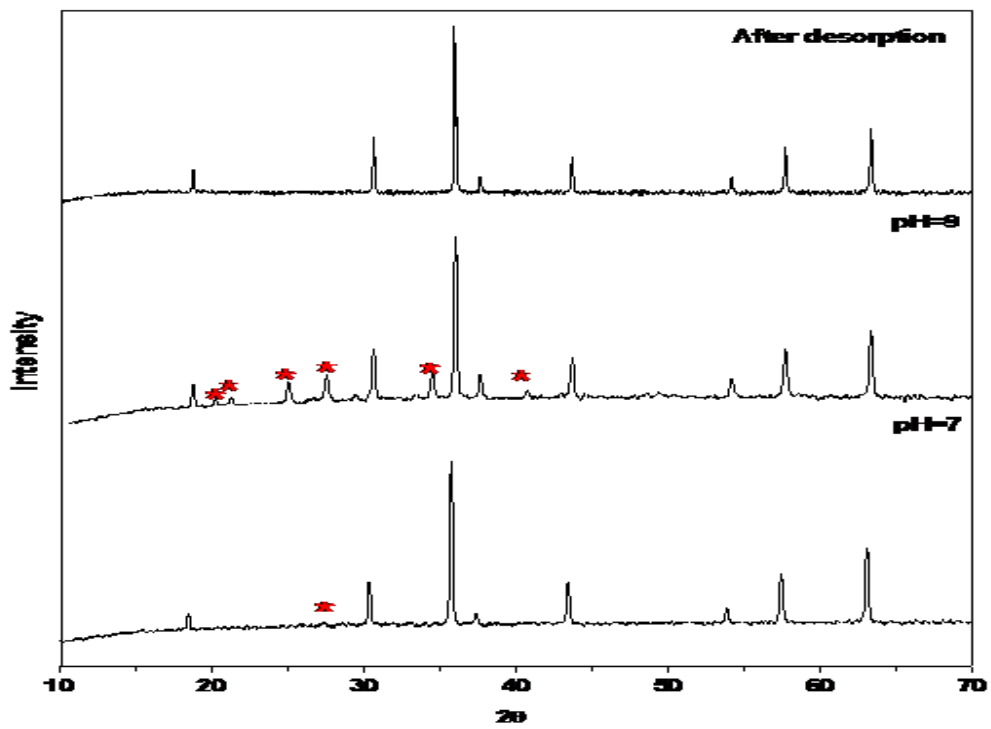
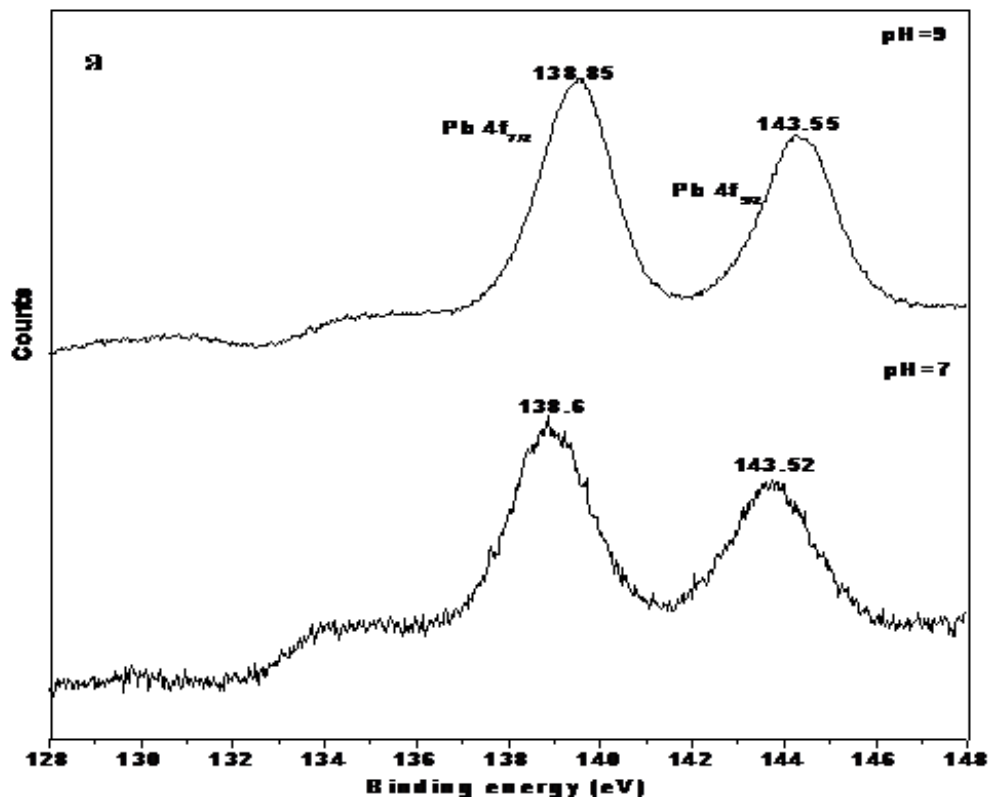


Fig.3



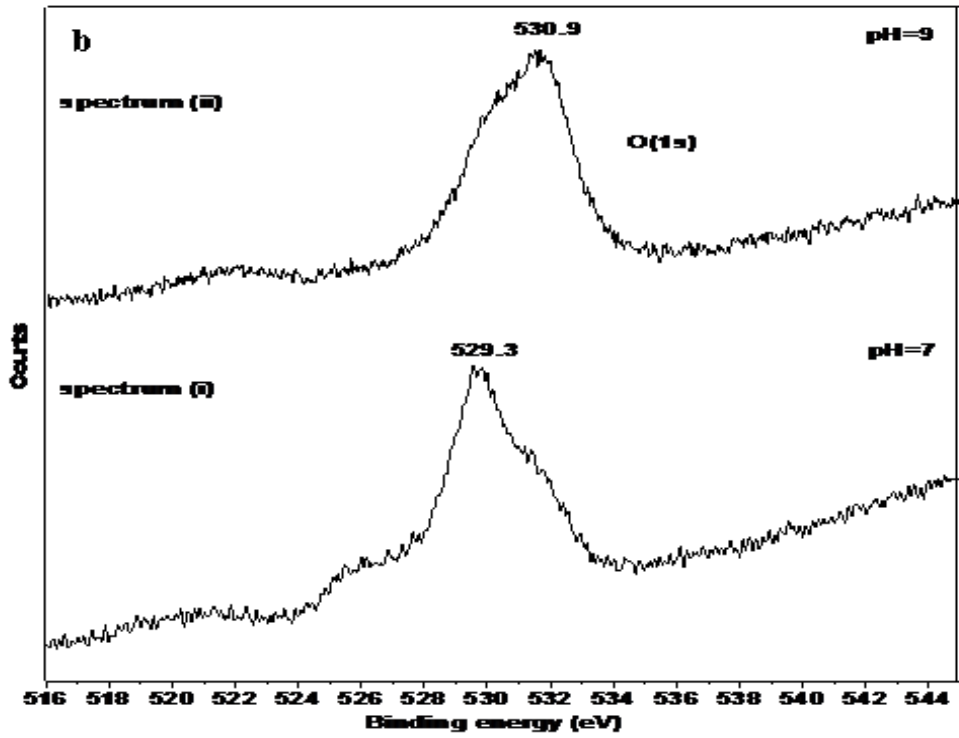


Fig 4

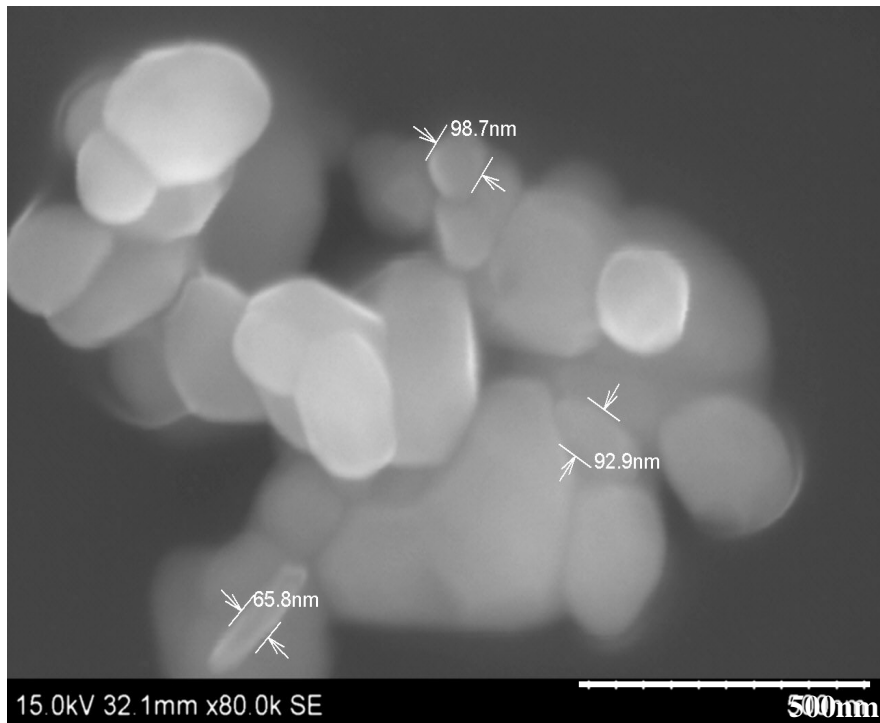


Fig 5

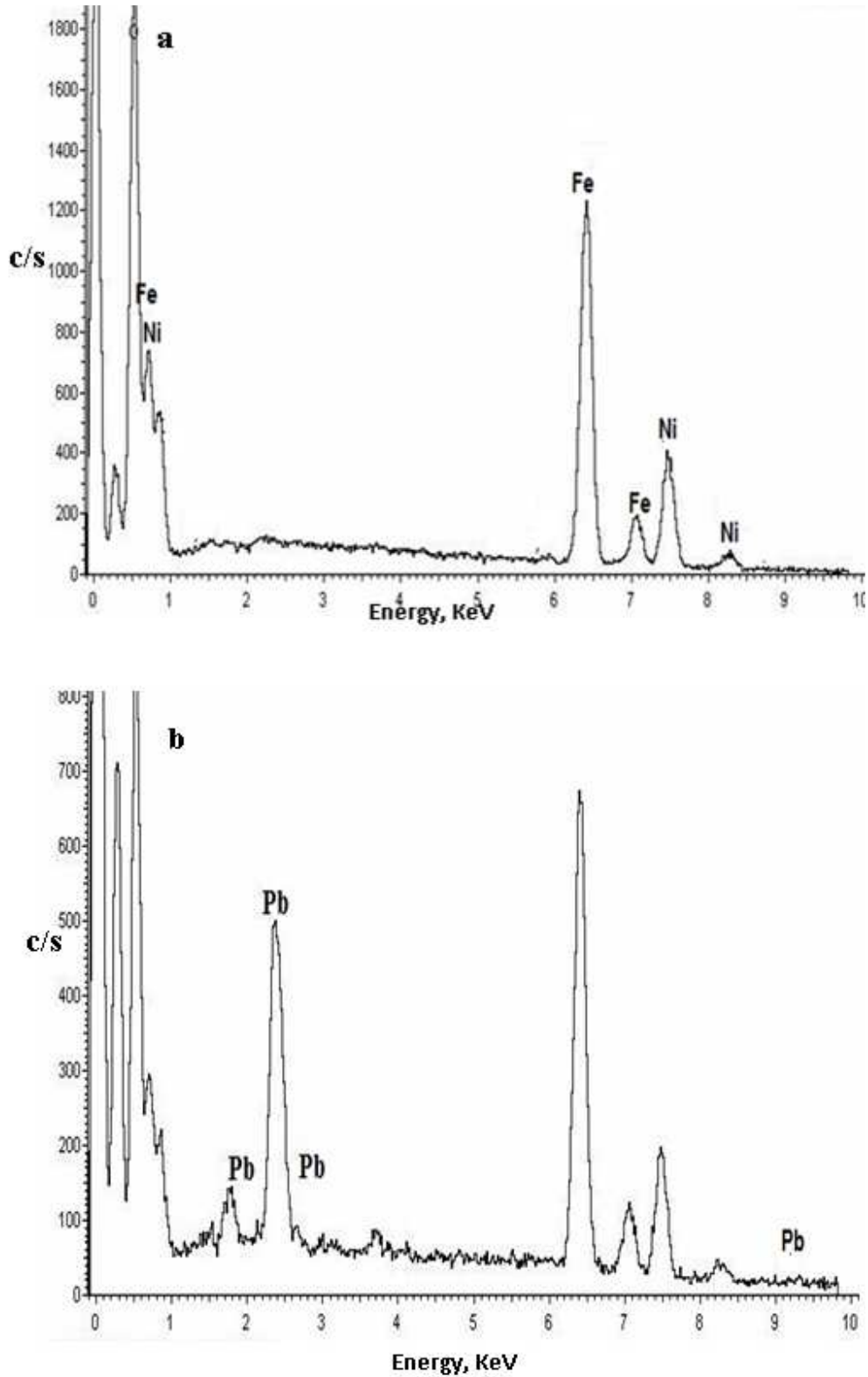


Fig 6

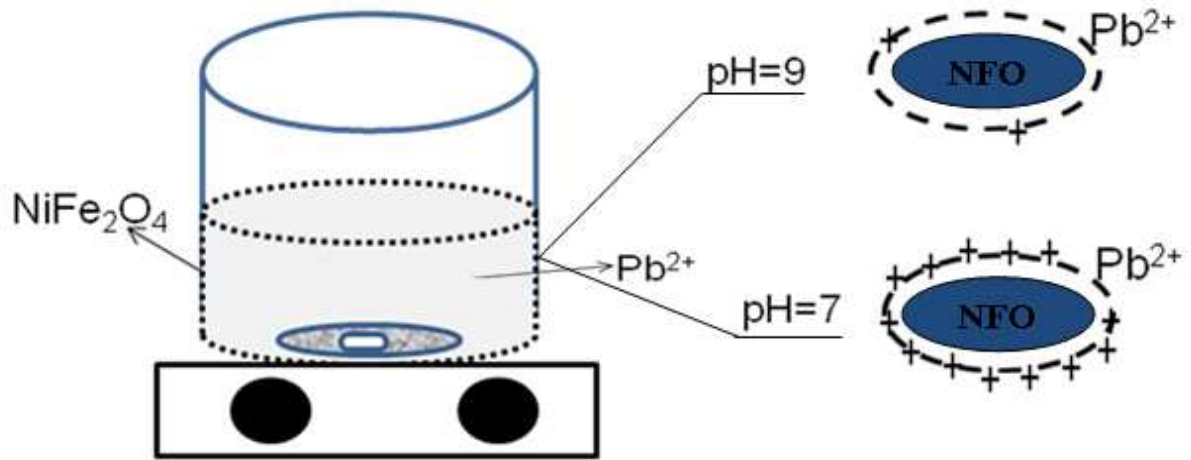


Fig 7